

Cell tracking with TRACE3D—a new algorithm

Jan Handwerker*

*Institut für Meteorologie und Klimaforschung, Universität Karlsruhe, Forschungszentrum Karlsruhe,
Technik und Umwelt, Postfach 3640, 76021 Karlsruhe, Germany*

Received 16 April 2001; accepted 15 July 2001

Abstract

An automated algorithm called TRACE3D is presented which identifies convective cells and tracks them in time and space by exclusively using radar reflectivity data as input.

Identification of cells is performed by assembling contiguous regions that excel certain reflectivity thresholds. Tracking is done in that the position of a cell in a new radar image is predicted by an extrapolation procedure based on its former position; special care is taken in case of possible splitting and merging events. In comparing the results of the tracking algorithm with those from four test persons, TRACE3D shows a promising performance, and hence, it seems possible to apply this algorithm as a nowcasting tool. © 2002 Elsevier Science B.V. All rights reserved.

1. Introduction

The high temporal and spatial resolution of continuous radar measurement provides not only snapshots of rain intensity (Eulerian point of view) but also contains valuable information on the dynamics of the development of convective cells (Lagrangian point of view).

In concentrating on tracking of convective cells, which can appear as single entities as well as in cluster (e.g. in a squall line), the most important issues are (i) the separation of these objects from the background and (ii) to retrieve them in subsequent images.

First tracking algorithms using radar data have been published in the 1970s. Rinehart and Garvey (1978) developed a correlation method (TREC) to find a certain pattern in the next volume scan. This procedure avoids the identification and isolation of discrete objects within a precipitation pattern. TREC uses a 2D product as input data and determines

* Tel.: +49-7247-82-2847; fax: +49-7247-82-4742.

E-mail address: jan.handwerker@imk.fzk.de (J. Handwerker).

motion vectors on a regular grid. It is applicable on convective precipitation as well as on stratiform events.

The regularity of the grid the motion vectors are determined on was used by Li et al. (1995) to improve the results by constraining the two-dimensional flow field which has zero divergence. Although this assumption cannot easily be substantiated by the dynamics of convective systems, the calculated motion vectors seem to be much more reliable.

Focusing on the evolution of discrete objects, a second group of algorithms has been developed (e.g. SCIT (Johnson et al., 1998) and TITAN (Dixon and Wiener, 1993)). These algorithms first identify specific objects within a single radar data set and try to find the same objects in the next data set again. The objects have to be small compared to the total volume seen by the radar, and pronounced enough to be clearly detachable from the background. TRACE3D is a new algorithm of this second type.

These identification and tracking algorithms define a storm cell as a contiguous region of high reflectivity values which outranges a certain minimum size. The specific algorithm method, however, differs from algorithm to algorithm. SCIT uses several distinct thresholds (30, 35, 40, ..., 60 dB_Z) to define objects, and in each elevation the reduced to its most intense region. TITAN applies a single threshold that is chosen by the user. The objects identified by TITAN differ evidently with respect to the chosen threshold.

The algorithm presented in this paper, TRACE3D, uses a first threshold to dissect the total radar image into separate “regions of intense precipitation” (called ROIP hereafter). Within each ROIP, the threshold that is used to define the convective cells depends on the maximum reflectivity in the ROIP (cf. Section 3.1).

After identification of cells, the second step is the retrieval of these objects within the next radar image. Within TITAN, a cost function is defined that takes into account the distance between the former and the recent position as well as the difference in volume of the cells. Minimizing this cost function gives the assignments between the objects. Additional effort is needed to treat splitting and mergings.

SCIT uses the velocity of the cells during former time steps in order to extrapolate the position of an individual cell to the recent time and searches in the vicinity of this predicted position for successors of the cell.

This is the basic idea of the tracking routines of TRACE3D as well. However, a more sophisticated procedure is used to deal with splittings and mergings.

TRACE3D is developed to investigate radar data with the aim to study the growth and decay of individual thunderstorms. It is proven to deal successfully with rather small objects. This gives the opportunity to observe thunderstorms already at a very early stage of development. The principal aim of TRACE3D is to reveal the impact of orography on thunderstorms, typical tracks of thunderstorms, and regions where thunderstorms are initiated or where they preferentially dissipate.

It should be noted that tracking of convective cells is not only performed on radar data but as well on data of lightnings, satellite data and output of numerical models. There are automated nowcasting systems that use several sensors to feed a numerical model with the aim not only to track existing thunderstorms but to predict initiation. An excellent overview on the nowcasting of thunderstorms is given by Wilson et al. (1998).

2. Input data

TRACE3D uses only radar data. This makes it easy to utilize the algorithm on any radar without the need of external data (as temperature profile, etc.) and without customization.

The most important input data are the (polar) reflectivity data. Clearly most radar data are contaminated by ground clutter, bright band and attenuation effects, etc. However, it is presumed here that the radar data have been corrected by a separate algorithm prior to a use by TRACE3D. Note that there are only some very simple routines within TRACE3D to avoid worst errors caused by incorrect input data as will be discussed in the next section.

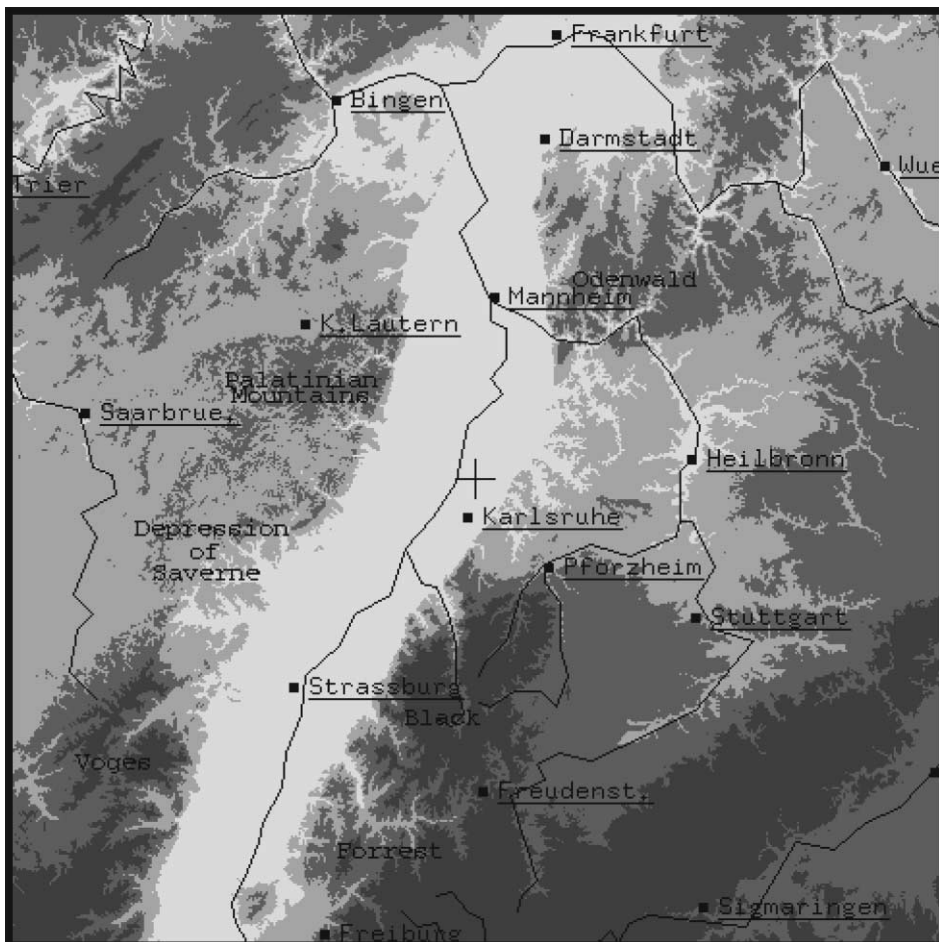


Fig. 1. Orography around the radar of the Forschungszentrum Karlsruhe. Radar position is denoted by the '+' in the center. The length of each edge is 240 km. The grey scales indicate heights a.s.l. <200, 200–350, 350–600, > 600 m.

If the radar has a Doppler capability, the VVP data (Waldteufel and Corbin, 1979) are helpful to give the first cells an initial velocity. So, in case VVP data are available, TRACE3D makes use of them, but they are not necessary for the algorithm.

The radar data for testing TRACE3D are from the radar of the Forschungszentrum Karlsruhe. The radar site is in the upper Rhine valley in Germany (8°26' 13" E; 49°5' 33" N, 148 m a.s.l., 38 m a.g.l.) which is stamped by a pronounced orographical structure. The southern part of the upper Rhine valley (about 100 m a.s.l.) is surrounded by the Vosges in the west (up to 1000 m a.s.l.) and the Black Forest in the east (up to 1200 m a.s.l.). The northern region of the Palatinatian Forest (west) and the Odenwald (east) reach up to 700 m a.s.l (see Fig. 1 for details). It is well known that this orography channels the surface winds (Fiedler, 1983), and therefore, it is quite likely that orographic impacts on the growth and decay of storm cells might be observable in this region.

The radar hardware (a C-band Doppler radar manufactured by the German company Gematronik) is identical to the radars of the German and the Swiss weather services (DWD and SMA). It performs a scan modus which is repeated every 10 min. In August 1999, we changed the scan strategy to optimize the data basis on which TRACE3D is working. The old schedule was:

- A 14-elevation volume scan of reflectivity and Doppler velocity with a range of 120 km, a range gate length of 500 m, dual prf (1200 and 800 Hz). The elevations are 0.4°, 1.1°, 2.0°, 3.0°, 4.5°, 6.0°, 7.5°, 9.0°, 11.0°, 13.0°, 16.0°, 20.0°, 24.0°, and 30.0°.
- A ppi of reflectivity (single prf) with a range of 300 km at 1.0°.
- A four-elevation precipitation (only reflectivity, single prf) scan using only the first four elevations of the volume.

In August 1999, the four-elevation precipitation scan is expanded to all 14 elevations used by the volume scan. Thus, each 10 min, two (nearly) identical volume scans are performed.

3. The algorithm

As stated above, TRACE3D works in two steps. First, cells are identified and then tracked. These steps are described in Sections 3.1 and 3.2. Each step consists of two smaller parts: a main part working in most cases, and an additional part, dealing with exceptions and more complicated structures.

3.1. Identification of reflectivity cores

3.1.1. Defining reflectivity thresholds

This cell-tracking algorithm only uses the reflectivity values to identify storm cells. The results are necessarily afflicted with errors. This is due to several effects. First, especially if one wants to detect rather weak convective cells, there are other meteorological echoes

that reach the same reflectivity values as these weak cells. Precipitation with 45 dB_Z is not necessarily a thunderstorm. Second, the reflectivity within the bright band reaches comparable values. So, it is not easy to distinguish between bright band and convective cells by only using reflectivity. Third, the reflectivity measurements suffer from ground clutter and from noise and so on. Fourth, due to attenuation, the reflectivity is often underestimated, thus thunderstorms might be overseen.

A fifth problem is the separation of cells. What is—in terms of reflectivity values—the differences between two individual cells which are closely adjacent to each other and one (larger) cell with two maxima? As long as one has to define a convective cell using thresholds, one cannot overcome artifacts. Sometimes, a large storm will be identified as two or more small objects and vice versa.

Thus, there is a difference between a real storm cell and those objects any algorithm identifies as a storm cell. To emphasize this difference, the term “reflectivity core” (abbreviated RC) will be used in the following for those objects TRACE3D identifies as cells.

The simplest way to define RCs might be to consider every beam volume element which exceeds a certain threshold (e.g. 35 dB_Z, in the following denoted as DBZ_{LIMIT}) and merge them to contiguous objects (cf. Fig. 2(a)). However, in situations of strong convection, this often leads to very large objects which obviously comprise of several individual cells. For example, a squall line of more than 150-km length, which was observed in the afternoon of June 7, 1998, is identified as a single RC by this procedure. It is impossible to study the individual behavior of a convective cell using this simple approach. This is one reason why the old tracking algorithm on the WSR-88D system, which used a single threshold, was replaced by SCIT, an algorithm that uses several fixed thresholds to find the core of a convective cell (Witt and Johnson, 1993; Johnson et al., 1998).

An improvement would be to reduce the above defined RCs to their relative maxima and their adjacency. This introduces a second threshold (DBZ_{DIFF}, typically 10 dB). Starting with a relative maximum within the reflectivity data that exceeds DBZ_{LIMIT} + DBZ_{DIFF}, all adjacent beam volume elements are added to the RC which are less than DBZ_{DIFF} lower than the maximum (cf. Fig. 2(b)). However, sometimes this procedure produces artefacts. Secondary maxima “grow” into their adjacent primary maximum as can be seen with RC 5 in Fig. 2(b).

To avoid this effect, a third method is used by TRACE3D. In a first step, the radar volume is dissected into “regions of intense precipitation” (ROIP) by the first threshold DBZ_{LIMIT} (cf. Fig. 2(c)). Note that these ROIPs are identical to the RCs defined in the simplest method (cf. Fig. 2(a)). Within each ROIP, the maximum reflectivity is then determined. The RCs within each ROIP are now defined as contiguous regions with reflectivity values not lower than this maximum minus DBZ_{DIFF}. This means that all RCs within one ROIP are limited by the same lower limit of reflectivity, not by an individual lower limit (cf. Fig. 2(c)). The maximum reflectivity value within an RC has to excel the value DBZ_{LIMIT} + DBZ_{DIFF}, otherwise, the RC will be rejected.

This procedure is somehow similar to that used by SCIT, but it does not use several fixed thresholds (30, 35, 40, 45, 50, 55, 60, dB_Z) to find the core of a cell, but TRACE3D always tunes the lower threshold for the RCs.

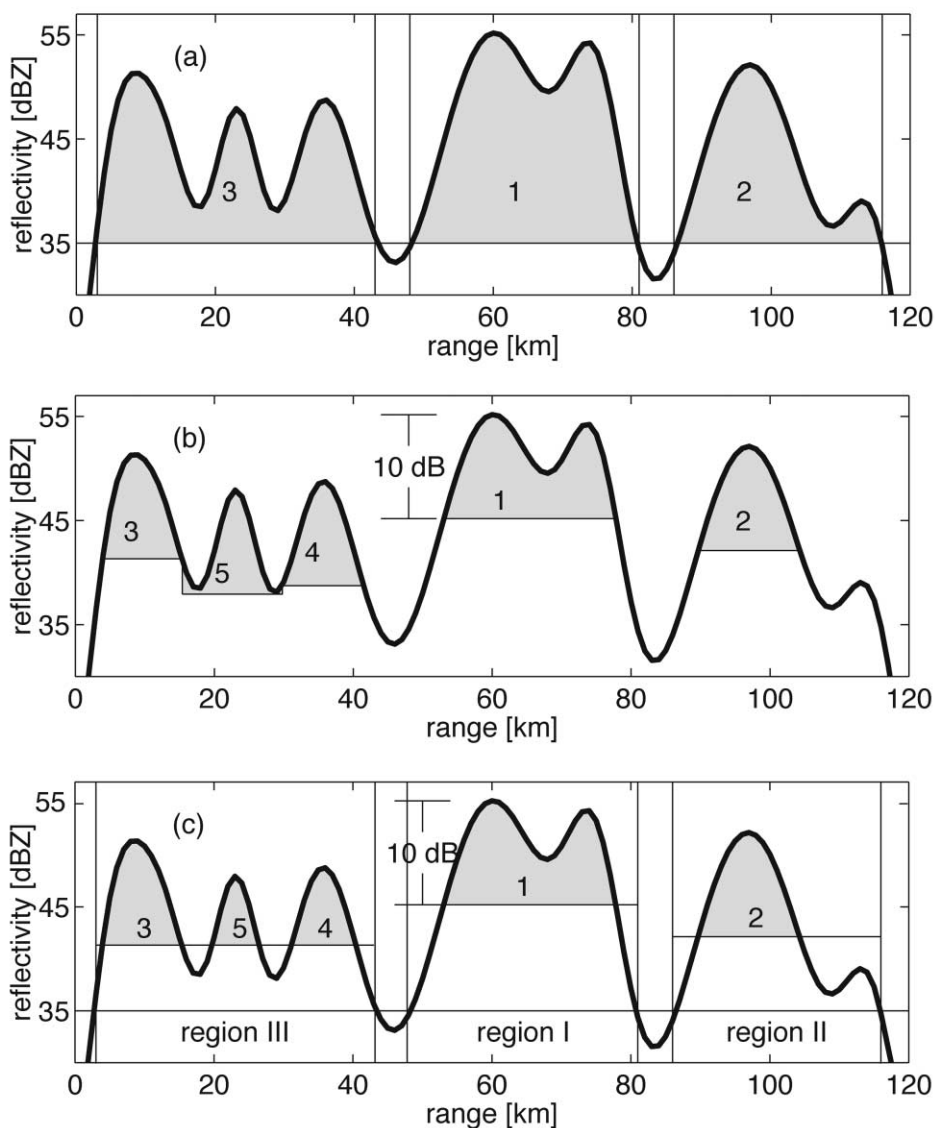


Fig. 2. Schematic sketch of possible methods to define reflectivity cores demonstrated on a unique one-dimensional data set. (a) Each beam volume element with a reflectivity above a certain threshold DBZLIMIT (35 dBZ) is part of an RC. (b) “The upper 10 dB” (DBZDIFF) are taken as RC. This might lead to RCs that include the lower regions of more prominent adjacent RCs as can be seen with RC 5. (c) In a first step, contiguous regions with a reflectivity value above a threshold (35 dBZ) are searched for. Within each region, a second threshold, 10 dB beneath the maximum reflectivity within that region, is used to define RCs. In this way, TRACE3D defines RCs.

Defining RCs this way produces unambiguous objects, avoiding the artifacts discussed above. However, it has to be mentioned that the volume of an RC depends on the maximum reflectivity value in its ROIP. If RC 3 in Fig. 2(c) was more intense (e.g. 55 dB_Z), RCs 4 and 5 became smaller.

Note that only the reflectivity values represent the seriousness of an RC. The volume is not a significant rating.

3.1.2. Fine tuning of RC detection

As mentioned above, radar data are affected by errors, introducing some difficulties for the identification of RCs. Thus, prior to the use in TRACE3D, the raw data from radar should be corrected. It is not the native task of a tracking algorithm to deal with data quality. Nevertheless, TRACE3D tries to consider some typical problems of radar data and applies very simple routines to prevent failures. These routines are as follows.

Ground clutter. Ground clutter is a common severe problem in radar meteorology and hence also in cell tracking algorithms, because clutter echoes are often intense (so they can be mixed up with convective cells) and stationary (so they represent objects with zero velocity, confusing the tracking algorithm). Ideally, input data should be free of ground clutter. Just to increase the degree of reliance a little bit, data below a certain height above ground (H_{MIN}, typically 1 km) are neglected.

Attenuation. Radar data suffer from attenuation effects. Especially in cases with convective precipitation, attenuation leads to an underestimation of rain reflectivity in the shadow of intense cells, whose correction is a difficult and yet unsolved problem far beyond the scope of a tracking algorithm. TRACE3D does not try to make a physical-based attenuation correction, but increases reflectivity values with respect to the distance to the radar according to a parameter called ATTKORR (typically 0.02 dB/km). According to Sauvageot (1992), this value corresponds to 3.6 mm/h (two-way attenuation) at C-Band wavelengths.

Combining nearby RCs. In the close vicinity of the radar, the spatial resolution is very fine. Together with noise, this produces sometimes so many small RCs which are obviously components of one larger RC. Even in far distance, RCs are cut in fragments by obstacles like chimneys which are close to the radar. To eliminate both effects, RCs which reside close to another are merged if their smallest distance remains under a certain value in meters (DMERGE_{MAXM}, typically 1000 m) or under a certain distance in beam volume elements (DMERGE_{MAXP}, typically two beam volume elements).

Neglecting peanuts. To eliminate data from aeroplanes, anaprop echoes, very small RCs are neglected. Again, two different thresholds are defined: (i) the number of beam volume elements has to exceed a lower limit (N_{MIN}, typically 3) for an RC as well as (ii) the area covered by the RC has to exceed A_{MIN} (typically 2 km²). These are a rather low thresholds compared with those used in other cell tracking algorithms (e.g. SCIT, TITAN), so nearly each meteorological object is accepted.

Detecting bright band. Bright bands have a very small vertical extent compared with convective cells. The chance of a false interpretation of a bright band as a convective cell is reduced by demanding that an RC has to be seen in at least two different elevations at at least a certain fraction (i.e. DOUBLE_{MIN}, typically 10%) of its area. Because of the fine

resolution, this is a very lax criterion in the vicinity of the radar, whereas at a large distance, it is quite strict.

All RCs which fulfill all of the above mentioned criteria are stored and tracked as described in the next section. In Table 1, all thresholds used for the identification of RCs are listed.

3.1.3. Calculating significant parameters describing reflectivity cores

For further investigations, the reflectivity values of each beam volume element of the RC are stored as an excerpt from the volume data in a special format. Strictly speaking, all reflectivity data between the smallest and the largest azimuth, the nearest and the farthest range bin, and all elevations are stored. Those reflectivity data belonging to the RC are marked. This offers the opportunity to calculate each parameter that might be of any interest for future examination. Besides these reflectivity data, the following parameters are routinely calculated and stored.

- The position of the nearest left corner (seen from the radar) and the size of an RC.
- The center of an RC given as:

$$\vec{r} = \frac{\sum w_i \vec{r}_i}{\sum w_i},$$

where w_i is a weight for the i th beam volume element and \vec{r}_i is its position. The weighting factors can be the reflectivity, the rain intensity, the logarithmic reflectivity or even unity. TRACE3D uses the logarithmic reflectivity as weights, but experience shows that it makes no significant difference for practical purposes which weight is used.

- The resolution of radar data in radial and azimuthal direction.
- The elevation angles of the scan.
- The number of the ROIP an RC belongs to.
- The total number of beam volume elements comprising an RC.
- Date and time.

Table 1
Thresholds used for identification of reflectivity cores

Name	Typical value	Unit	Description
DBZLIMIT	45	dB _Z	maximum reflectivity has to excel this value
DBZDIFF	10	dB	maximum difference between the maximum reflectivity of the RC and an accepted adjacent beam volume element
HMIN	1000	m	minimum height above ground a valid reflectivity value has to be measured at
ATTENKORR	0.02	dB/km	global attenuation correction
DMERGEAXM	1000	m	maximum distance of two beam volume elements of two different RCs to be merged
DMERGEAXP	2	pixel	same as DMERGEAXM but in pixels
NMIN	3	pixel	minimum number of beam volume elements of an RC
AMIN	2	km ²	minimum area of an RC
DOUBLEMIN	0.1	–	fraction of the area of an RC where it has to be observed at least two elevations

Fig. 3 shows an example of detected RCs. As can be seen, even rather weak objects are identified as RCs. For most RCs, the 45-dB_Z echotop is below 4 km and the maximum reflectivity value is less than 50 dB_Z, the smallest RC covers less than 2 km².

If these small RCs are of no interest, they can be easily neglected by increasing the threshold dB_ZLIMIT. This improves the quality of the tracking routines because less objects will be found. However, if we want to study the total life cycle of an RC, we have to take it into account already in its premature stage. Nevertheless, one can disregard all those thunderstorm that do not reach a certain reflectivity threshold during their total life cycle afterwards.

3.2. Tracking of reflectivity cores

After identification of RCs within a certain volume scan, TRACE3D tries to assign the RCs of the former volume scan to those of the recent scan. Tracking is, of course, performed only if in the predecessor scan and in the successor scan RCs are detected. If the time lag between two successive scans exceeds a certain value (DT, typically 30 min), e.g. because of a malfunction of the radar, no tracking is applied. Otherwise, the assignments would be rather stochastic.

The philosophy of the tracking is as follows: Let us assume we can estimate a velocity for each RC. First, each parent RC¹ is moved according to its velocity and the given time step to an estimated position. Potential children might be found in the later scan near this estimated position. Afterwards, it is checked whether parent and child fit in size in a certain sense. If not, a splitting or merging might have taken place and it is looked for extra parents or children. This procedure tends to find all reasonable assignments between parents and children—but unfortunately, it tends to find more assignments than reasonable. Banning crossings of RC tracks reduces the assignments in most cases very well. Only in situations with a high density of RCs additional reductions have to be performed. Here is the procedure in detail.

3.2.1. Extrapolation

The most important step during the tracking procedure is the estimation of the position of the tracked RC at time t of the new data set. For this purpose, we have to estimate a velocity $\vec{v}_c(t)$ for each RC within the parent data set. TRACE3D tries the following approaches to give each RC its velocity.

3.2.1.1. The core has been tracked before for one time step. This means we have observations of this storm at times $t - 2\delta t$ and $t - \delta t$, where δt is the time interval between

¹ In the following, the terms *parent* and *child* are used to give a short, intuitive description of the temporal order. In fact, a parent RC and a child RC are two observations at two different times of the same thunderstorm. Sometimes, even RCs from the former scan are called parents although they do not have children (dissipating storms), and RCs from the recent scan are called children although they do not have parents (initiating storms). So, the figure of parents and children is not perfect, but it is intuitive and hence it is used.

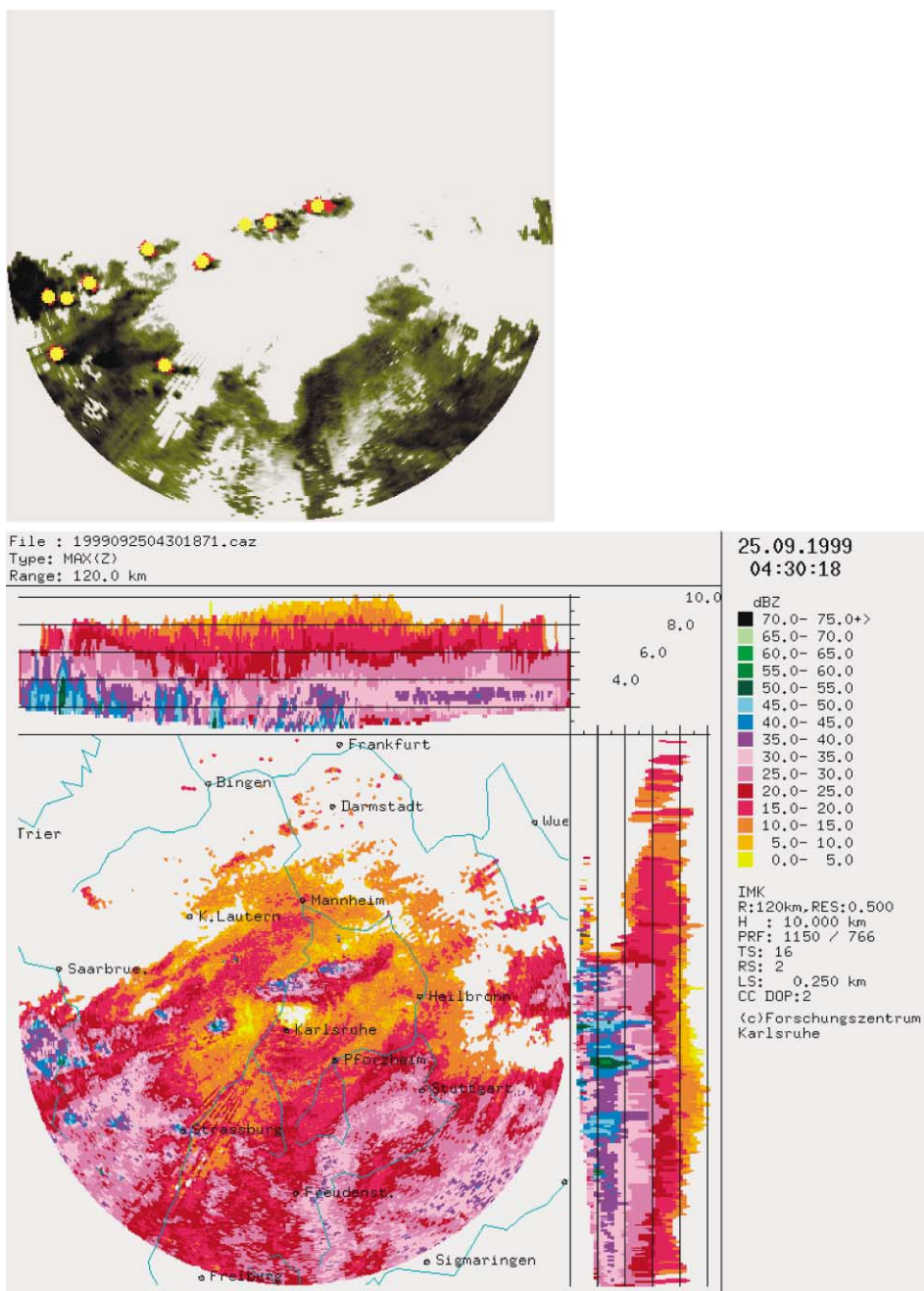


Fig. 3. Example of detected RCs within a radar image. The yellow crosses denote the centers of RCs, the red dots mark all beam volume elements corresponding to that RC. The grey code indicates surface rain intensity. On the lower picture, the corresponding maximum projection reflectivity image (Sep. 25, 1999, 4:30 LT) is shown.

two radar scans. From these observations, we know the positions $\vec{r}_m(t - 2\delta t)$ and $\vec{r}_m(t - \delta t)$, so we can calculate a measured velocity by:

$$\vec{v}_m(t - \delta t) = \frac{\vec{r}_m(t - \delta t) - \vec{r}_m(t - 2\delta t)}{\delta t}.$$

We take this measured velocity from the former time step as the estimated velocity of this time step ($\vec{v}_e(t) = \vec{v}_m(t - \delta t)$).

3.2.1.2. The core has been tracked before for more than one time step. In this case, the estimated velocity can be calculated as a weighted sum of all former measured velocities. This can be expressed by the recursive formula:

$$\vec{v}_e(t) = k \vec{v}_e(t - \delta t) + (1 - k) \vec{v}_m(t - \delta t).$$

The parameter k determines the rate at which old information become unimportant. Varying k between 0.5 and 0.9 does not influence the results essentially. With $k=0$, only the last measured velocity is used, discarding all older information (Handwerker et al., 2000). We use $k=0.7$ as a standard.

3.2.1.3. The core is new born. A new born RC, i.e. an RC without an assigned predecessor, is initiated with the averaged velocity of all other RCs that got predecessors within the parent data set.

If there are no other RCs with predecessors, the averaged velocity calculated by the volume velocity processing (VVP) algorithm in heights between 2000 and 4000 m above the radar is used (Waldteufel and Corbin, 1979).

3.2.1.4. There is no velocity available at all. In very seldom cases, even the velocity from the VVP algorithm is not available. In these cases, there are nearly always only very few RCs within the range of the radar. Then, the nearest RC in the next data set is assumed to be the successor of an RC, as long as the velocity remains smaller than 15 m/s, which means that the slowest possible motion to reach a child RC is taken as a first approach.

Using these velocity estimates, one gets an estimated position of the parent RC at the time of the child volume scan. The true position is assumed to be in the vicinity of that position. All RCs in the child volume scan are taken into account as child RCs as long as their distance to the estimated position is smaller than a certain search radius (cf. Fig. 4). This search radius is given by the larger of the following two distances:

1. the (estimated) distance an RC moved during this time step, i.e. $|\vec{v}_e(t)|\delta T$ multiplied by VELOCITYFACTOR, a free parameter chosen by the user (typically 0.6), or
2. the distance to the next neighbor of a parent RC in the parent volume scan multiplied by NEXTNEIGHBORFACTOR (typically 0.5), where the distance to the neighbor must not be larger than DRMAX (typically 10 km), otherwise DRMAX will be taken.

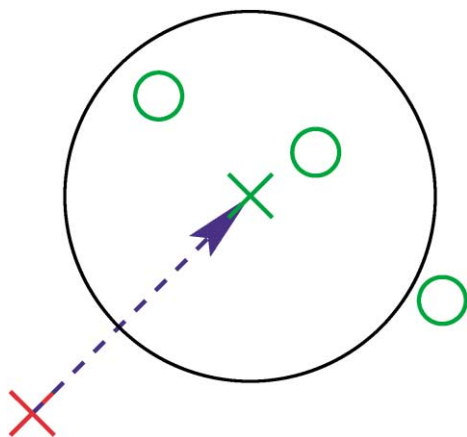


Fig. 4. Principal part of tracking. The green cross marks the estimated position of an RC that was observed at the red cross in the former radar image. The green circles are RCs observed in the recent radar image. The two circles within the search radius (black circle) are taken into account as candidates for childhood.

The first radius reflects that the absolute precision of the estimation of the next RC position depends on the distance the RC travels during one time step. In cases of very slow isolated cells, the second length allows a generous search radius. Each RC within the search radius is considered to be a candidate for childhood for a parent RC.

Up to this stage, the result is a matrix of assignments, which connects the parent RCs with RCs in the next radar image.

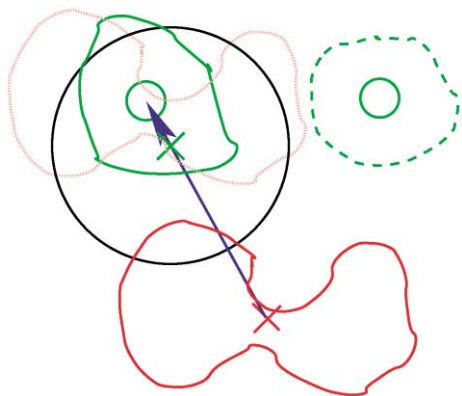


Fig. 5. Identification of splittings. To identify splittings, the parent RC (red) is moved to the position of identified child RC (solid, green). The covered area of the moved parent (dotted, red) is compared to the area of the child.

3.2.2. Fine tuning of cell tracking

In simple cases, the described procedure is sufficient to get the right assignments from parents to children RCs. Additional routines try to improve the results in more delicate situations.

3.2.2.1. Splitting and merging. In nature, cell splitting are spectacular events, which might be observed by radar and are valuable to investigate. However, as long as one uses thresholds to define certain objects within a radar data set, splittings as well as merging occur as artifacts. Nevertheless, we have to identify these cases as well, to get the right assignments between RCs. This is done by the following procedure.

Splittings. To detect a splitting, the complete parent RC is moved to the position of its (yet found) child. If there is more than one child, the parent RC is moved to the volume weighted center of all children. Then, the area covered by the (moved) parent is compared with that covered by its (yet found) child (cf. Fig. 5). If both areas are comparable, there is no reason to assume that a splitting took place. However, if the child is very small compared to the parent, a splitting is likely.

To compare the areas of parent and child, it is looked for regions of the (moved) parent that are more than $DS_{PLITTMIN}$ (typically 2000 m) apart from the child. If those regions can be found, it is looked for other RCs within the child radar image, whose center is closer to these regions than the distance the parent RC moved in this time step. If there are such RCs, they are additionally taken into account as a candidate for childhood.

In Fig. 5, the parent RC (solid red line) is moved to the position of its only child. The areas of the moved parent (dashed red line) and the child (solid green line) do not compare well. There are two regions (left and right) which are not represented by the area of the child. If we can find a beam volume element within these regions, which is farther than 2 km apart from the child, we should assume a splitting. As can be seen, there is no further cell on the left side to the child, but there is one to the right side. Although the cell to the right is not within the search circle (black), it is now taken as a candidate for childhood. For human eyes, it is obvious that the cell split into two smaller parts.

To reduce the amount of calculations in large RCs (consisting of many beam volume elements), only a subset of NP_{MAX} (typically 200) randomly chosen beam volume elements are used during this calculation.

Mergings. To identify mergings, the same calculation as for splittings is performed in the opposite direction: The child is moved to the center position of all parents. If there are beam volume elements of the moved child which are more than $DS_{PLITTMIN}$ apart from the nearest beam volume element of the parent RC, another parent is searched as described above.

3.2.2.2. Ban of crossings. The described procedure is designed to accept assignments rather very freehanded than being too fussy. In a next step, the less credible assignments will be rejected.

It is not really impossible that the route of a certain RC is crossed by another route of another RC during a time step. This could happen without an interpenetration of the RCs

when the two RCs are at that cross point at different times within the time step. Nevertheless, such a crossing is surely a rather seldom event, so it should be a good assumption that there is something wrong with the assignments as long as there are crossings.

Therefore, it is calculated which assignments between parent and child RCs lead to crossing if we assume a linear motion of the RCs during an individual time step. As a result, all RCs that might suffer a crossing are selected as a group and all RCs connected via assignments with these RCs gathered (cf. Fig. 6, top left). For each group, the averaged velocity is calculated (red arrow). Now, successively the assignment best corresponding to the averaged velocity is accepted (green line, top right) and those assignments producing crossings with it are rejected (brown lines, top right). This process is repeated until an already rejected assignment would be accepted (then all remaining assignments which lead

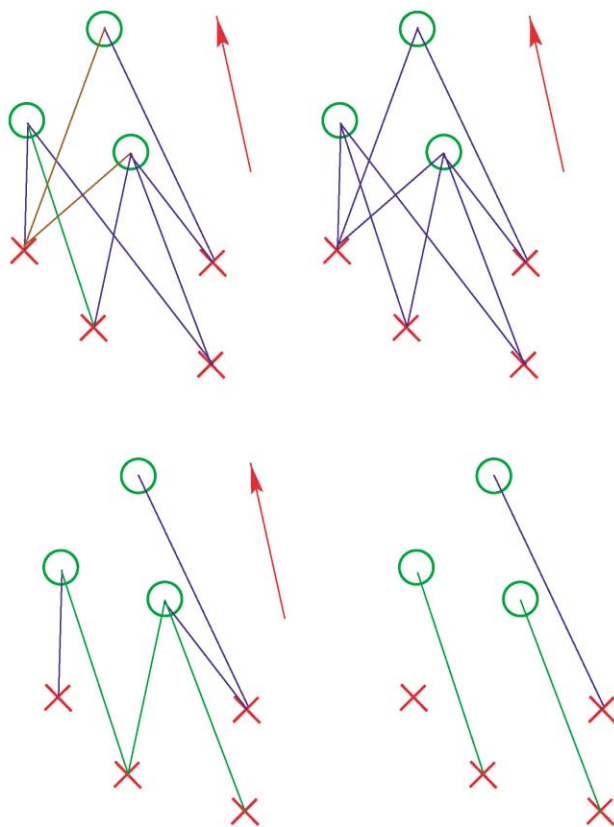


Fig. 6. Removal of crossings. Crosses mark the positions of parent RCs, circles the positions of child RCs. Assignments corresponding with the average velocity (red arrow) are accepted (green line, upper right), assignments which cross the accepted ones are removed (brown line, upper right). If there remain still more than three parents and more than three children (lower left), splitting and merging is forbidden. Only the assignments corresponding best with the average velocity are accepted (lower right).

Table 2
Parameters used for the tracking of reflectivity cores

Name	Typical value	Unit	Description
DT	1800	s	maximum time lag on which tracking is performed
NPMAX	200	–	maximum numbers of beam volume elements representing a RC for splitting/merging analysis
DSPLITMIN	2000	m	minimum distance to be splitted of
DRMAX	10000	m	maximum distance to a neighbor
NEXTNEIGHBORFACTOR	0.5	–	factor for the radius of the search radius
VELOCITYFACTOR	0.6	–	factor for the radius of the search radius

to crossings are rejected) or until no crossings are left. This process ends normally up with a situation sketched in the lower left of Fig. 6.

3.2.2.3. Defining heaps of reflectivity cores. In most cases, the assignments are acceptable at this point of processing. However, when several RCs are getting very close together—e.g. in a squall line—tracking gets nearly impossible, as can be seen by visual observation. As growth and decay, splitting and merging of individual cells are fast compared to the time span between two scans, the assignments will be arbitrary.

A measure to separate cases where tracking will be successful and those where it will not is given by the ratio of the distance an RC moves during a time step and the distance between an RC and its neighbor within a single radar image. Thus, increasing the temporal resolution of the volume scans improves the results of tracking algorithms. In these cases, where even visual inspection will fail, the best information the algorithm can report is that its result are no longer reliable.

To identify these situations, TRACE3D calculates the number of parent and child RCs interconnected by assignments to a group. If one group contains three or more parent RCs and three or more child RCs, this group is called a “heap of RCs”. Within a heap, a regular assignment is difficult. The detection of mergings or splitting is even more difficult. Thus, within a heap of RCs, no splitting and no merging is allowed. Each parent is only allowed to have one child and vice versa.

Again, the averaged velocity according to all assignments of a heap is calculated and the assignments are accepted in the order of their consistence with that averaged velocity (cf. Fig. 6, lower right). These assignments are marked so that it is possible to reconstruct the existence of a heap afterwards.

The assignments calculated with this routine are stored. All parameters used to track the RCs are summarized in Table 2.

4. Checking the performance

To get an impression of the performance of the tracking algorithm presented so far, we compared the results of TRACE3D with those determined by eye. To this end, four persons were shown the positions of identified RCs superimposed on the surface rain intensity (cf. Fig. 3).

Table 3
Cases used for evaluation

Date	Time	Temporal resolution (min)	Average no. of RCs per image
07.04.99	14:04–19:34	10	6
13.06.99	11:04–15:54	10	16
30.06.99	6:34–9:44	10	19
05.10.99	13:00–17:00	5	6
25.09.99	4:00–6:40	5	12
31.10.99	0:00–1:50	5	27

For each case, the temporal resolution and the average number of RCs per image is given.

We chose six time sequences, three of them with a temporal resolution of 10 min and three with 5-min resolution (cf. Table 3). The three sequences with equal temporal resolutions differ with respect to their average number of RCs per image. As long as there are only a few RCs (say 10) per radar image, tracking is rather easy. With very many RCs per image (say more than 20), tracking is hard.

The four persons as well as the algorithm TRACE3D produced five data sets of assignments. From these data sets, a sixth one is calculated as described below, which is called “the truth”: An assignment is said to be correct if and only if three or more of the five data sets contain it. This means that TRACE3D is involved in defining the truth. In cases where two persons believe an assignment to be correct and two do not, the result of TRACE3D is assumed to be correct independent whether or not TRACE3D believes this assignment to be correct. As can be seen from the results below, the human eyes worked very similar so the contribution of TRACE3D to the truth is not significant.

On the other hand, this definition of the truth allows to qualitatively measure the data sets of the test persons and take their results for comparison purposes.

Comparing each of the five individual data sets of assignments with the “truth” data set, we can get four different findings:

Hit. An assignment is found in the individual data set and in the “truth” data set. This is called a hit (*h*).

Table 4
Tracking results distinguished for the three different situations with a temporal resolution of 10 min as given in Table 3

Date	Tracked by	POD	FAR	CSI
07.04.99 (easy)	TRACE3D	0.94	0.04	0.91
	test persons (average)	0.97	0.06	0.91
13.06.99 (medium)	TRACE3D	0.90	0.04	0.87
	test persons (average)	0.98	0.04	0.94
30.06.99 (hard)	TRACE3D	0.93	0.09	0.85
	test persons (average)	0.96	0.04	0.92
Average (10 min resolution)	TRACE3D	0.93	0.05	0.89
	test persons (average)	0.97	0.05	0.92

Table 5

Same as Table 4 but for the three cases with a temporal resolution of 5 min

Date	Tracked by	POD	FAR	CSI
05.10.99 (easy)	TRACE3D	0.97	0.01	0.96
	test persons (average)	1.00	0.00	0.99
25.09.99 (medium)	TRACE3D	0.92	0.04	0.88
	test persons (average)	0.96	0.03	0.93
31.10.99 (hard)	TRACE3D	0.87	0.07	0.81
	test persons (average)	0.97	0.03	0.94
Average (5 min resolution)	TRACE3D	0.94	0.03	0.91
	test persons (average)	0.98	0.01	0.96

Miss. An assignment is not found in the individual data set although it is found in the “truth”. This is called a miss (m).

False alarm. An assignment is found in the individual data set although it is not found in the “truth”. This is a false alarm (f).

No event. An assignment is neither found in the individual data set nor in the “truth”.

With these definitions, we calculated three different indices of success: the probability of detection ($\text{POD} = h/(h+m)$), the false alarm rate ($\text{FAR} = f/(h+f)$) and the critical success index ($\text{CSI} = h/(h+m+f)$). In the optimum, POD and CSI reach 1 and FAR is 0. Calculating these parameters seems to be an objective method to evaluate tracking algorithms. It has to be emphasized that a comparison between different tracking algorithms is hardly possible as long as they use different objects to track and strike for different goals (Wilson et al., 1998).

The benchmarks of TRACE3D are given in Tables 4 and 5. For each of the six cases, the three different indices of success are given. TRACE3D as well as the test persons get better marks in easy cases than in hard cases. The algorithm seems to be more sensitive to the severity of tracking than human beings are. In total, the algorithm performs worse than the test persons. Nevertheless, the results of the TRACE3D are encouraging.

To calculate the average performance of the algorithm within 1 year, we have to look at the frequency distribution of the number of RCs within one radar image, which indicates the severity of tracking given in Table 6. This statistic is based on all radar images of 1999 which contained precipitation. (Radar images without precipitation are purged regularly.) Roughly 30% of these images contain RCs. More than 50% of all RCs occur within easy situations, i.e. within images with 10 or less RCs. Only in 1% of all images, more than 20 RCs appear, but they reflect 14% of all RCs.

Table 6

Distribution of the number of RCs within one radar image

RCs per image	Percentage of pictures (%)	Percentage of RCs (%)	Severity
0	70	0	–
1–10	25	54	easy
11–20	3	32	medium
21 or more	1	14	hard

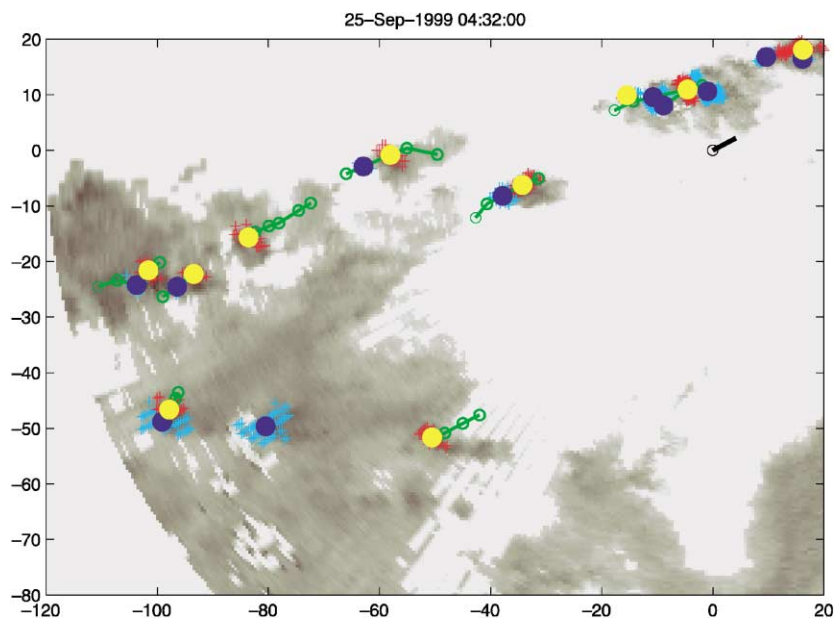


Fig. 7. Example of the results of TRACE3D. For details, see text.

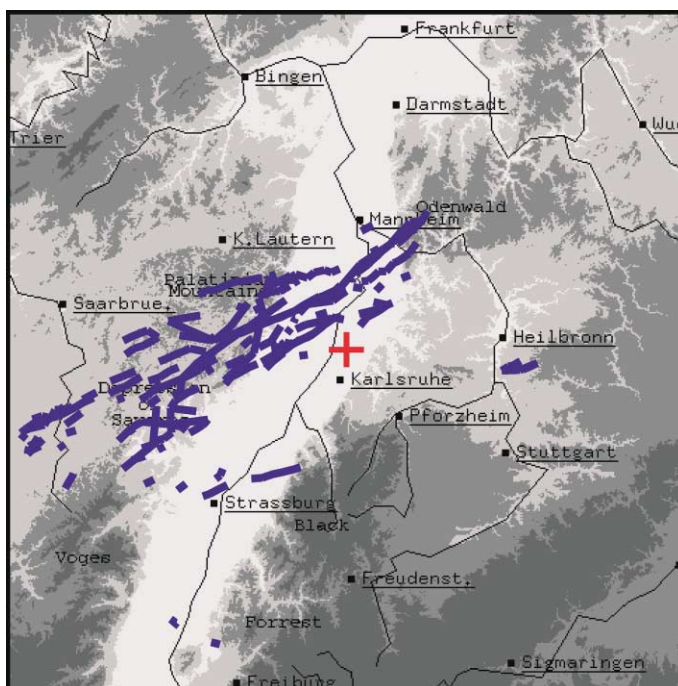


Fig. 8. All tracks observed from 4:00 LT to 6:30 LT, Sep. 25, 1999.

Taking the results from the benchmark test as representative for the easy, medium and hard cases (which is reasonable but not proven approach), average performance indices are calculated for both temporal resolutions. The results concerning a certain degree of severity are weighted with the frequency of reflectivity RCs during periods with the severity as given in Table 6.

On the basis of 5-min input data, the probability of detection is just 6% from perfection and the false alarm rate is only 3%. These results are very satisfactory.

5. An example

To give an impression of the results provided by TRACE3D, the evaluation of some data from Sep. 25, 1999 is presented here. These data are part of one of the six data sets that were used for evaluation purposes and were already shown as Fig. 3. The tracks of these RCs are depicted in Fig. 7. The positions of the RCs at 4:30 LT are marked with yellow dots. The area covered by the RCs is denoted by the red '+'. The positions and areas of all RCs within the former radar image (4:25 LT) are marked by the blue dots and cyan '+'. Earlier and later positions of these RCs are given by the green circles. The time delay between two circles is 5 min.

There are 11 RCs observed at 4:25 and 10 RCs at 4:30. They move from WSW to ENE. The black line at the position of the radar (0,0) denotes the wind speed from the VVP algorithm measured at 4:30 LT (average between 2000 and 4000 m) multiplied with the time step (5 min). It matches the velocity of the RCs acceptable.

For example, it is seen that the RC at position 80 km west and 18 km south from the radar is new born (there is no blue dot connected to it), and it exists for five time steps (25 min). During this time, it moves to 70 km west and 10 km south from radar. The RC at position 80 km west, 50 km south from the radar was observed in the last image but is not seen in the recent image (no yellow dot). The RC 3 km west, 8 km north from radar has got two predecessors (two blue dots west of it). So, here, one can see a merging event.

All tracks observed that morning are plotted in Fig. 8. As can be clearly recognized, most thunderstorms travelled from the depression of Saverne (that is the depression nearly amidst a line from Saarbrücken to Straßburg) to the Odenwald (east of Mannheim). This track is supposed to be a prominent storm track in the upper Rhine valley, which shall be proven or disproven using TRACE3D. This is left to future investigations.

6. Summary

An algorithm called TRACE3D has been presented by which convective cells (i) can be identified and (ii) tracked in space and time by evaluating radar reflectivity data only. In order to adapt the cell definition to a large variety of cases individual thresholds of radar reflectivity, values are chosen in each radar image.

The future position of a cell is estimated from information on the location and speed of former times. By a special procedure, possible cell splittings and mergings are accounted for.

A comparison of results obtained independently by some test persons and application of TRACE3D exhibits an encouraging performance of that algorithm.

It should be emphasized that TRACE3D can also handle rather small object which is necessary to observe the formation of the thunderstorms already at an early premature stage.

The only input data TRACE3D needs and relies on are polar raw reflectivity data. This makes the algorithm applicable to every weather radar with very limited need of customization. If the radar provides Doppler information, the VVP-Profile will be used by the algorithm.

Finally, it should be noticed that TRACE3D gives access to the temporal development of several properties of thunderstorms, e.g. reflectivity, vertical profile, position, velocity and so on. These information are essential for an analysis of the impact of orography on convection.

TRACE3D is available as source code for free. If you are interested, please contact the author.

Acknowledgements

Sincere thanks are given to Prof. Dr. Klaus D. Beheng for initiating the development of TRACE3D and for critical proofreading of this article that improved the text significantly. I have benefited greatly from his support and many discussions with him, not only on convection. Julia Ressing, Axel Seifert and Ulrich Blahak have to be thanked for tracking the RCs by eye.

References

- Dixon, M., Wiener, G., 1993. TITAN: thunderstorm identification, tracking, analysis, and nowcasting — a radar-based methodology. *J. Atmos. Oceanic Technol.* 10, 785–797.
- Fiedler, F., 1983. Einige Charakteristika der Strömung im Oberrheingraben. *Wiss. Ber. Meteorol. Inst. Univ. Karlsruhe*, no. 4, 113–123.
- Handwerker, J., Reßing, J., Beheng, K.D., 2000. Tracking convective cells in the upper Rhine valley. *Phys. Chem. Earth (B)* 25, 1317–1322.
- Johnson, J.T., MacKeen, P.L., Witt, A., Mitchell, E.D., Stumpf, G.J., Eilts, M.D., Thomas, K.W., 1998. The storm cell identification and tracking algorithm: an enhanced WSR-88d algorithm. *Weather Forecast.* 13, 263–276.
- Li, L., Schmid, W., Joss, J., 1995. Nowcasting of motion and growth of precipitation with radar over a complex orography. *J. Appl. Meteorol.* 34, 1286–1300.
- Rinehart, R.E., Garvey, E.T., 1978. Three-dimensional storm motion detection by conventional weather radar. *Nature* 273, 287–289.
- Sauvageot, H., 1992. *Radar Meteorology*. Artech House, Boston.
- Waldteufel, P., Corbin, H., 1979. On the analysis of single doppler data. *J. Appl. Meteorol.* 18, 532–542.
- Wilson, J.W., Crook, N.A., Mueller, C.K., Sun, J., Dixon, M., 1998. Nowcasting thunderstorms: a status report. *Bull. Am. Meteorol. Soc.* 79, 2079–2099.
- Witt, A., Johnson, J., 1993. An enhanced storm cell identification and tracking algorithm. 26th International Conference on Radar Meteorology. American Meteorological Society, Boston, MA, Norman, Oklahoma, pp. 141–143.